J Electroceram (2009) 23:410–414
DOI 10.1007/s10832-008-9479-1

Morphology and luminescence properties of $BaMgAl_{10}O_{17}:Eu^{2+}$ blue phosphors by Aerosol Flame Deposition

Sang Won Ko · Dongwook Shin

Received: 28 May 2007 / Accepted: 18 March 2008 / Published online: 2 May 2008

Abstract $BaMgAl_{10}O_{17}:Eu^{2+}$ (BAM:Eu) is widely used as a blue phosphor for fluorescent lamps and plasma display panels (PDP). The improvement of the luminescence efficiency is a significant issue for applications in plasma display panels. In this study, the Aerosol Flame Deposition (AFD) was applied to fabricate $BaMgAl_{10}O_{17}:Eu^{2+}$ (BAM:Eu) particles with spherical shape and fine size in order to improve their luminescence. The sub-micrometer powder was synthesized in spherical shape in an oxy-hydrogen flame and deposited on a substrate in the form of porous film. The particle size of as-prepared powder increased with increasing the concentration of precursor solution and the heat treatment under reducing atmosphere increased particle size additionally with surface roughening due to the needle-like crystallized phases. Photoluminescence spectrum was observed at about 450nm due to the 5d–4f transition of Eu^{2+} and the intensity of phosphor was as high as 70% of that of the commercial phosphor.

Keywords PDP · Phosphor · BAM · $BaMgAl_{10}O_{17}:Eu^{2+}$ · Aerosol Flame Deposition

1 Introduction

Flat panel displays (FPD) have come into the spotlight in the display market due to lightweight, small volume and high definition image. Plasma display panel (PDP) is one of the representative flat panel display which has great potential for the wall hanging High Definition Television (HDTV) because the large sized display could be produced at relatively low cost. Moreover, it offers a wide viewing angle, a fast response and small volume [1].

In general, numerous parameters, such as the morphology and particle size, the composition and stoichiometry, the chemical stability, and the microstructure of the particle surface, play important roles in the performance of the final phosphor powder [2]. Phosphors for plasma display panel are required to possess high absorption cross section to the radiation at wavelength of 147nm and 172nm, chemical and physical stability under VUV light, suitable decay time and high luminescence.

$BaMgAl_{10}O_{17}:Eu^{2+}$ (BAM:Eu) is widely used as one of the most important blue phosphor for fluorescent lamps and plasma display panels because of its high efficiency and chromaticity that is corresponding to a broad band around 450nm due to the transition from $4f^6 5d^1$ to $4f^7$ of divalent europium ions under vacuum ultraviolet (VUV) radiation from an inert gas plasma(147nm, 172nm) [3–5].

It is generally known that fine particle size and homogeneous morphology improve luminescence by enhancing to form compact phosphor layer and spherical particles shape with smooth surface also improves by reducing the scattering of light emitted from phosphor. Therefore, the control of morphology of phosphor particle has been recognized as one of the important engineering approach to improve the luminance efficiency under VUV. $BaMgAl_{10}O_{17}:Eu^{2+}$ particles synthesized by conventional solid state reaction synthesis methods exhibit plate-like morphologies and commercial phosphors produced by this

S. W. Ko · D. Shin (✉)
Division of Materials Science and Engineering,
Hanyang University,
17 Haengdang-dong, Seongdong-gu,
Seoul 133-791, Korea
e-mail: dwshin@hanyang.ac.kr

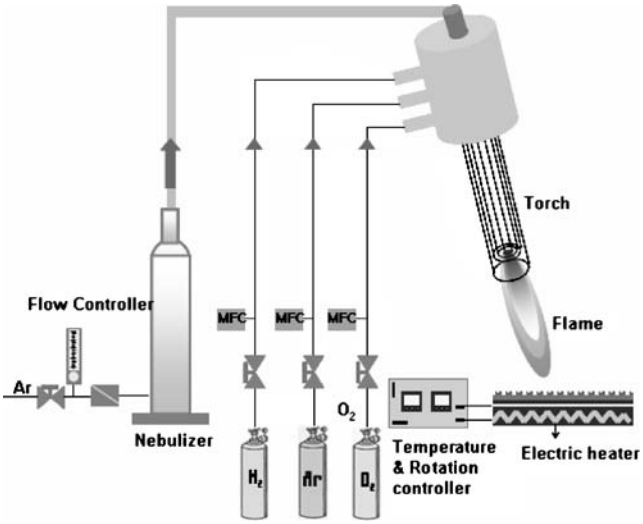

Fig. 1 A schematic diagram of Aerosol Flame Deposition apparatus for the synthesis of BAM

method generally are composed of large and irregular-shaped particles [6]. Hence, to improve luminescence of synthesized powder phosphor, numerous methods have been applied to control its plate-like morphology [7–9].

In this study, the Aerosol Flame Deposition (AFD) was applied to fabricate phosphor particles with spherical shape and smooth surface to improve their luminescence. AFD is a method to synthesize ultra-fine oxide particles as demonstrated in optical fiber and integrated optical waveguide devices [10]. In AFD process, source materials in the form of gas phase or liquid phase atomized into aerosol are fed into an oxy-hydrogen torch where the aerosol droplets undergo condensation and oxidation into precipitate particles. Due to very high temperature of oxy-hydrogen flame and short reaction time, it is a very effective process to produce multi-component oxide materials with a stoichiometric composition. In general, this technique has number of advantages in terms of the choice of precursors, the crystallinity and shape of produced powder, the simplicity of process and potential for the mass production due to high synthesis efficiency [11]. In the study, the $BaMgAl_{10}O_{17}:Eu^{2+}$ powder with spherical and non-agglomerated particle for PDP application were prepared by employing AFD and the general characteristics of powder will be reported.

2 Experimental

The precursor materials for the preparation of $BaMgAl_{10}O_{17}:Eu^{2+}$ phosphors were $Ba(NO_3)_2$ (Rieddel-Dehaen, >99%), $Mg(NO_3)_26H_2O$ (Sigma-Aldrich, >99%), Al $(NO_3)_39H_2O$ (Riedel-Dehaen, >99%), $Eu(NO_3)_35H_2O$ (Fluka, >98.5%). The doping concentration of Europium as activator was 10atm.% of barium component to optimize for maximal luminescent intensity [12]. Precursor solutions were prepared by dissolving precursor chemicals in stoichiometric ratios into distilled water and mixed ultrasonically until clear solutions were obtained. The atomized precursor solution was delivered by a flow controller to the oxy-hydrogen torch. A schematic diagram of the experimental setup is shown in Fig. 1 which basically consists of a gas distribution unit, a precursor supply unit, a combustion unit, a sample support unit, and a temperature control unit. A flow controller supplies the solution into the combustion unit. Gas pressure and flow rate were controlled by flowmeter controller. The oxy-hydrogen torch system is the combustion unit, which is made from four concentric tubes, creating three gaps, and outer shield tube which is able to keep flame stable. Precursor solution flows

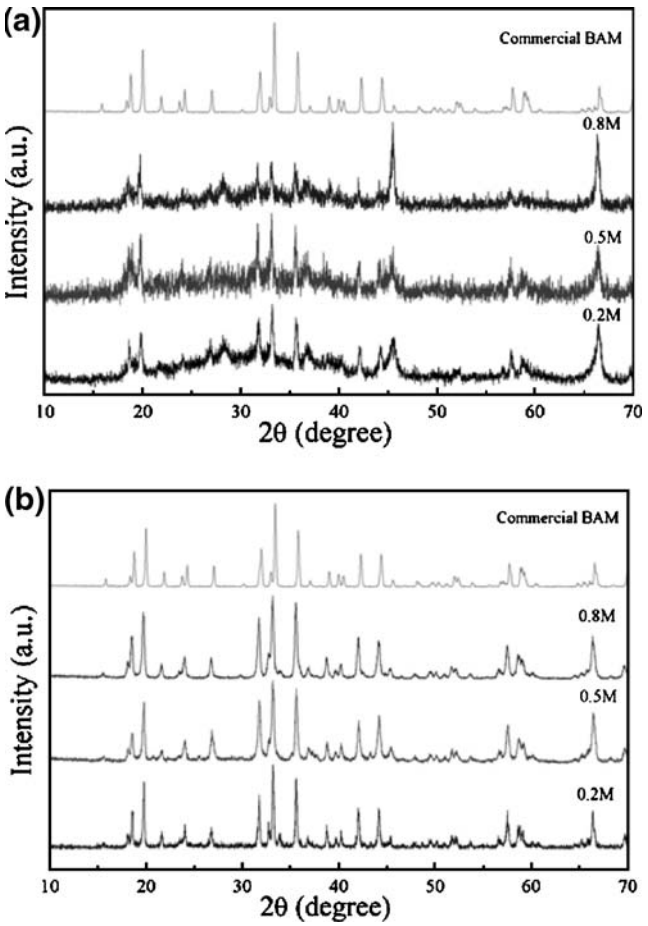

Fig. 2 XRD patterns of BAM:Eu^{2+} phosphor at various precursor solution mole concentration with fixed hydrogen gas flow rate of 3.0 L/min and oxygen gas flow rate of 7.5 L/min. (**a**) Before heat treatment and (**b**) after heat treatment at 1400 °C for 3 h in 5% H_2/Ar atmosphere

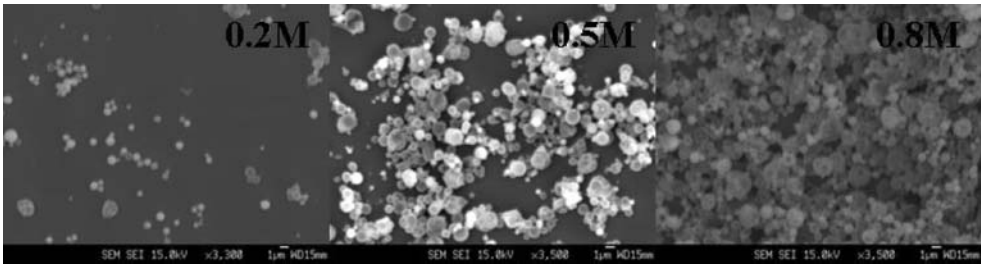

Fig. 3 SEM images of BAM powders synthesized by AFD at various precursor solution mole concentration with fixed hydrogen gas flow rate of 3.0 L/min and oxygen gas flow rate of 7.5 L/min

through the tube in the center of the torch while hydrogen, argon and oxygen were supplied through three gaps. The precursor solution atomized by 1.7Mhz ultrasonic nebulizer was fed into the oxy-hydrogen torch where the aerosol droplets undergo evaporation, oxidation and condensation of the precipitate particle in the submicron size range. The flow rate of Ar carrier gas was 1L/min. For control of substrate temperature, the substrates are heated on the turntable in which resistance heating element is embedded. The deposition temperature was controlled by heating the turntable and adjusting oxy/hydrogen flow rate. The prepared particles were heat treated at 1400°C for 3h under reducing atmosphere of 5mol% H_2/ 95% Ar mixtures for increasing crystallinity of particle and activating of divalent europium.

The crystallinity of the particles was characterized using an X-ray diffractometer (XRD). Scanning electron microscopy (SEM) was used to identify the particles sizes and morphology of the particles.

The photoluminescence spectra of the BAM particles were measured in vacuum under ultraviolet emission (147nm) excitation and compared to that of commercial BAM phosphor.

3 Results and discussion

Figure 2 shows XRD patterns of prepared BAM particles and heat-treated BAM particles. High background intensity and weak peak intensity in XRD pattern of as-prepared powder suggests that the prepared BAM:Eu^{2+} powder contains appreciable amount of amorphous phase. Similar patterns were observed regardless of deposition conditions. However, the heat treatment under reduction atmosphere improved dramatically the crystallinity of the prepared particles as shown in Fig. 2. The diffraction peaks of heat treated BAM sample were in excellent agreement with those of the standard BAM phase (JCPDS card 26-0163), which suggests that the pure phase BAM was obtained at lower heat treatment temperature than that of conventional solid-state reaction methods. It is well known that the luminescent intensity is affected by the phase purity of phosphor. The prepared powder did not include appreciable amount of impure phases.

Figure 3 shows the synthesized particles and the effect of the concentration of precursor solution on particle size. The smooth surface of synthesized particles suggests that the mechanism of particle formation is the condensation and precipitation. Particles are formed by the rapid evaporation of liquid solvent in high temperature flame and the

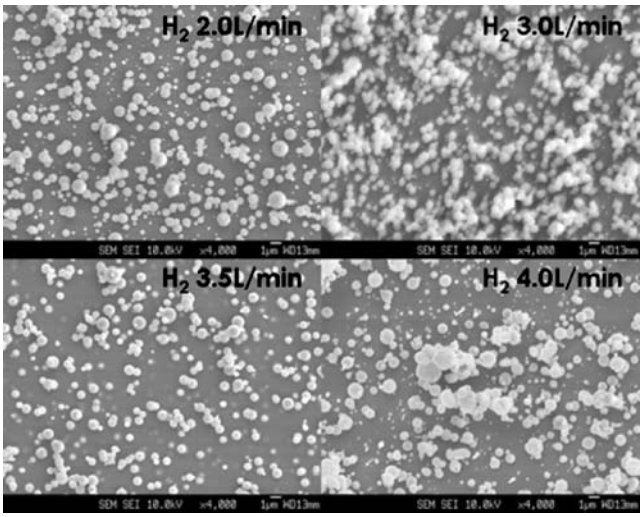

Fig. 4 SEM images of BAM powders synthesized by AFD at various hydrogen gas flow rate with fixed solution concentration of 0.8 M and oxygen gas flow rate of 7.5 L/min

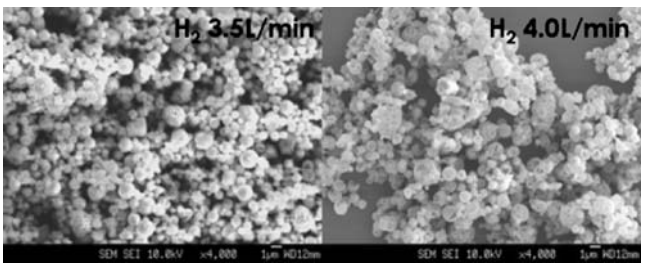

Fig. 5 SEM images of BAM powders synthesized by AFD after heat treatment under reducing atmosphere. Synthesis condition was identical to that of powder shown in Fig. 4. Heat treatment condition was 1400 °C for 3 h in 5% H_2/Ar atmosphere

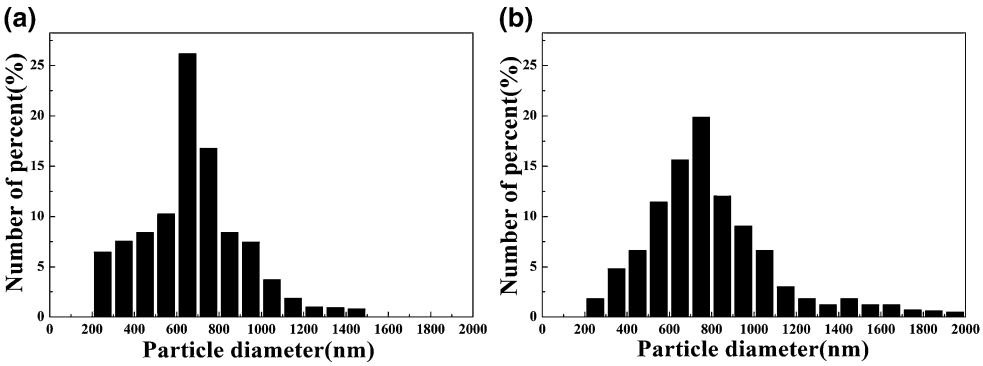

Fig. 6 Particle size distribution of AFD-synthesized BAM powders (**a**) before and (**b**) after heat treatment at 1400 °C for 3 h in 5% H_2/Ar atmosphere at hydrogen gas flow rate of 3.5 L/min with fixed solution concentration of 0.8 M and oxygen gas flow rate of 7.5 l/min

condensed precursor precipitates into solid particles. The size of particle formed by the condensation and precipitation mechanism is largely depending on the aerosol droplet size and the concentration of source liquid as predicted by Lang [13]. The particle size, d_p, is expressed by the Eq. 1;

$$d_p = \left[\frac{MC_s}{1000\rho_s}\right]^{1/3} D_{\text{droplet}} \quad (1)$$

where D_{droplet} is the droplet size of aerosol generated by ultrasonic nebulizer, M and ρ_s are the molecular weight and theoretical density of the particle material, and C_s is the concentration of source materials in the precursor solution. This theory predicts the slope in $\log(d_p)$ vs. C_s plot is 1/3 and the experimental data in this work produced the slope of ~0.31. This suggests that there are other parameters determining the particle size in the real experiments such as the change of the viscosity of precursor solution, breaking up of droplet, the coagulation of particles within the flame.

Figure 4 shows that the as-prepared particles have spherical shape with smooth surface and the particle agglomeration is fairly low. Increasing hydrogen flow rate turned out to exhibit a mild increase in particles size. Hydrogen gas generally increases the flame temperature and the increased temperature induces the increase of particle size through the inhomogeneous nucleation of plasma gas species on the surface of particle.

Heat treatment enlarged the particle size and roughened the surface by the crystallization as shown in Fig. 5. The average particle size of as-prepared particles was 670nm and that of heat-treated particles was 830nm. The needle-like crystalline phases were observed to roughen the surface of heat-treated particles (Fig. 6).

The photoluminescence characteristics of BAM:Eu^{2+} particles measured at room temperature under vacuum ultraviolet (147nm) excitation are shown in Fig. 7. The spectrum due to the 5d–4f transition of Eu^{2+} was observed at 450 nm. The intensity of phosphor is high as 70% of that of the commercial phosphor and the luminance of phosphor is high as 85% of that of the commercial phosphor. The lower intensity may be attributed to low tap density due to small particles size and partially to the rough surface induced by heat treatment. However, the color purity and chromacity were almost identical to those of commercial phosphor, suggesting that the purity of synthesized crystalline phase and basic particle characteristics are good enough to be utilized in the real application.

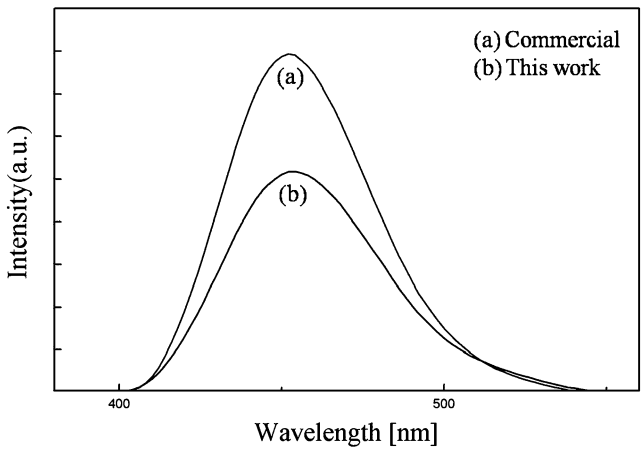

Fig. 7 Photoluminescence spectra of AFD-synthesized BAM powders at hydrogen gas flow rate of 3.5 L/min with fixed solution concentration of 0.8 M and oxygen gas flow rate of 7.5 L/min

4 Conclusions

Aerosol Flame Deposition was designed and applied to fabricate $BaMgAl_{10}O_{17}:Eu^{2+}$ phosphor particles with spherical shape as well as high phase purity. The heat treated BAM particles exhibited excellent crystallinity and the XRD peaks matched with the standard BAM phase. However, the optimizing the manufacturing process requires more sophisticated condition in order to fabricate dense BAM particles. It is apparent that the advantage of AFD is the capability of producing spherical particles and it helps the deposition of film with good homogeneity. The phosphor film made out of plat-like shape commercial particles had a rough structure whereas the film by AFD is expected to form a fine and close-packed layer.

Acknowledgements This work was supported by the Seoul Research and Business Development Program (Grant No.10583).

References

1. C.H. Kim, I.E. Kwon, C.H. Park, Y.J. Hwang, H.S. Bae, B.Y. Yu, C.H. Pyun, G.Y. Hong, J. Alloys Compd. **311**, 33–39 (2000)
2. A. Vecht, C. Gibbons, D. Davies, X. Jing, P. Marsh, T. Ireland, J. Silver, A. Newport, J. Vac. Sci. Technol. **17**, 750–757 (1999)
3. C.R. Ronda, J. Alloys Compd. **225**, 534–538 (1995)
4. T. Justel, J.C. Krupa, D.U. Wiechert, J. Lumin. **93**, 179–189 (2001)
5. G. Bizarri, B. Moine, J. Lumin. **113**, 199–213 (2005)
6. K.Y. Jung, D.Y. Lee, Y.C. Kang, S.B. Park, Korean J. Chem. Eng. **21**, 1072–1080 (2004)
7. L.T. Chen, I.L. Sun, C.S. Hwang, S.J. Chang, J. Lumin. **118**, 293–300 (2006)
8. H.K. Jung, D.W. Lee, K.Y. Jung, J.-H. Boo, J. Alloys Compd. **390**, 189–193 (2005)
9. Y.C. Kang, H.S. Roh, H.D. Park, S.B. Park, Ceram. Int. **29**, 41–47 (2003)
10. J.R. Bonar, M.V.D. Vermelho, P.V.S. Marques, A.J. McLaughlin, J.S. Aitchison, Opt. Commun. **149**, 27–32 (1998)
11. W.J. Stark, S.E. Pratsinis, Powder Technol. **126**, 103–108 (2002)
12. H. Chang, I. Wuled Lenggoro, T. Ogi, K. Okuyama, Mater. Lett. **59**, 1183–1187 (2005)
13. F.L. Yuan, C.H. Chen, E.M. Kelder, J. Schoonman, Solid State Ion. **109**, 119–123 (1998)